Modeling Surface Roughness-Related Uncertainties of Leaky Lamb Wave Clamp-On Ultrasonic Flowmeters

Xiaotang Gu and Frederic Cegla

***Abstract*— Transit time clamp-on ultrasonic flowmeters (UFMs) are widely used in industry due to their ease of installation. However, these ultrasonic clamp-on flowmeters are also known to be less accurate than ultrasonic inline flowmeters because of the uncertainties induced by the installation process. Amongst the installation-related parameters that influence the measurement uncertainties, internal pipe wall roughness is one of the most significant but uncontrollable parameters. The effect of roughness on accuracy can be reduced by operating the flowmeter at a longer wavelength. This article investigates the effect of roughness on a clamp-on UFM using low-frequency (200 kHz) leaky Lamb waves. This results in operation at roughly five times lower frequency compared with conventional clamp-on UFMs. The ultrasonic signals of this leaky Lamb wave UFM were simulated using the 2-D finite-element (FE) analysis. Using the simulated signals, the roughness effects on the uncertainties were quantified. The simulation results show that the uncertainty related to pipe wall roughness of leaky Lamb wave UFMs is approximately half that of conventional UFMs for corroded pipe walls with rms value larger than 0.1 mm (0.2, 0.35, and 0.5 mm). Demonstration experiments were also carried out to detect leaky Lamb wave using an electromagnetic acoustic transducer (EMAT). The experiment shows that the simulation correctly captures all the physics of the wave propagation and that we, therefore, can trust the simulation results with incorporated roughness.**

***Index Terms*— Clamp-on flowmeter, leaky lamb wave, roughness, transit time, ultrasonic, uncertainties.**

I. Introduction

TRANSIT time clamp-on ultrasonic flowmeters (UFMs) are widely used in many industries because they are non-invasive and easier to install compared with inline UFMs [1]. The installation of these clamp-on flowmeters only requires transducers to be mounted onto the outside of the pipe wall to transmit and receive an ultrasound, whereas inline flowmeters require cutting of the pipe and insertion of a spool piece. Fig. 1(a) shows a conventional clamp-on UFM. The bulk ultrasonic waves are transmitted from a transducer on one side of the pipe to another transducer on the other side of the pipe.

Manuscript received September 20, 2019; revised December 17, 2019; accepted February 9, 2020. Date of publication February 20, 2020; date of current version August 11, 2020. This work was supported by ASEA Brown Boveri (ABB). The Associate Editor coordinating the review process was Chao Tan. *(Corresponding author: Xiaotang Gu.)*

The authors are with the Non-Destructive Evaluation Group, Mechanical Engineering, South Kensington Campus, Imperial College London, London SW7 2AZ, U.K. (e-mail: f.cegla@imperial.ac.uk).

Color versions of one or more of the figures in this article are available online at http://ieeexplore.ieee.org.

Digital Object Identifier 10.1109/TIM.2020.2975389

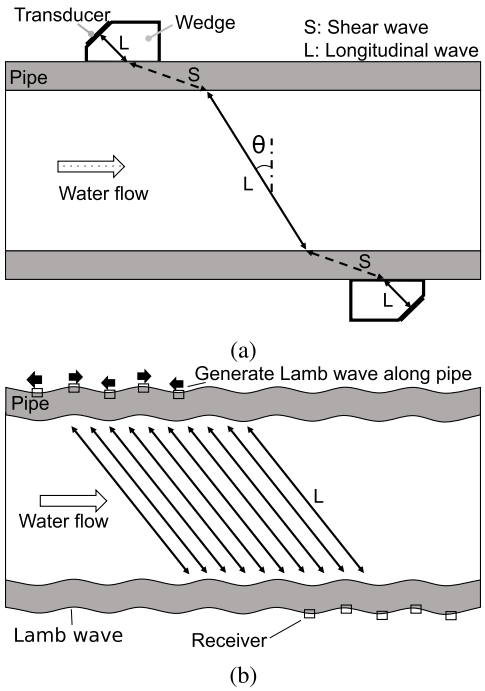

Fig. 1. Schematic of the cross-sectional view of a pipe filled with water. (a) Principle of conventional wedge type clamp-on UFMs. The ultrasonic waves transmit through the wedge, and water enters the pipe at an angle α (b) Leaky Lamb wave clamp-on UFMs. Lamb waves are generated along the pipe using interdigital transducers, and the Lamb wave continuously leaks energy into water at an angle.

The longitudinal waves from the transducer travel through a wedge into the pipe wall where they mode-convert to shear waves at the internal pipe wall surface. The shear waves then convert back to longitudinal waves in the fluid that is contained inside the pipe. These longitudinal waves traverse the pipe and travel to the receiving transducer via mode conversion to shear waves in the pipe wall and longitudinal waves in the receiving wedge.

Due to the existence of the flow, the signals that are sent downstream are accelerated, and the signals that are sent upstream are decelerated. The flow velocity is then measured by calculating the difference between the arrival time of the downstream and upstream ultrasonic signals.

The main drawbacks of these conventional clamp-on UFMs are the uncertainties induced by the installation process [2]. Amongst the installation-related parameters (pipe, wedge, and fluid properties) that influence the measurement uncertainties, internal pipe wall roughness is one of the most significant but

uncontrollable parameters [3]. The wave scattering due to the rough surface causes phase modulation and reduction in the amplitude of the signal and, therefore, reduces the accuracy of the measurements [4], [5]. Gu and Cegla [6] has discussed and quantified the effect of roughness due to wave scattering (nonflow profile-related effect). It shows that there could be as much as 2% accuracy error induced for a moderately corroded pipe (a typical moderately corroded pipe has an rms height of 0.2 mm [7]). This is, therefore, a substantial proportion of the overall uncertainty of the clamp-on UFM measurements, which is stated to be 1%–5% by most manufacturers. This overall uncertainty is a combination of all the sources of uncertainties, such as pipe thickness and wedge angles. In this article, the uncertainties due to other sources are assumed to be zero, and we only focus on the nonflow profile-related scattering of ultrasound at the internal pipe wall roughness.

One potential solution to reduce the effect of this uncontrollable parameter on accuracy is to operate the flowmeter at a longer wavelength using lower frequency. This is shown in several publications. For example, Benstock *et al.* [8] show that the ultrasonic thickness measurement error is proportional to the frequency.

As shown in Fig. 1(b), the method that is being investigated in this article is the use of the leaky Lamb waves at 200 kHz instead of the conventional clamp-on UFM at 1 MHz. This method generates low-frequency leaky Lamb waves (200 kHz) that continuously leak energy (in the form of longitudinal waves) into the fluid at an angle to the flow.

As shown in Fig. 1(b), if the leaky Lamb wave is generated on the top surface, the longitudinal waves in water are sent downstream and accelerated by the flow, while if the leaky Lamb wave is generated on the bottom surface, the longitudinal waves are sent upstream and decelerated by the flow. As a result, the arrival time of the received Lamb wave on the other side of the pipe is also accelerated and delayed, respectively. Calculating the difference between the arrival times of the received Lamb wave, the flow velocity can be measured. Fig. 1(b) shows the cross-sectional view of the pipe and water. In real life, the Lamb waves are generated around the whole circumference of the pipe, and the longitudinal wave propagation shown in Fig. 1(b) is axis-symmetric about the central axis of the pipe.

The idea of using Lamb waves in flowmetering is well-known. Publications dating back to 1985 [9], [10] report a thorough theoretical study of the principle. Furthermore, commercial applications are available in the form of thin-wall liquid flowmeters [11], [12]. However, there is no information readily available that quantifies the effect of pipe wall roughness on the uncertainties of this type of flowmeter.

This article aims to simulate this leaky Lamb wave method and to quantify the effect of roughness on the measurement accuracy of this method. The results are then compared with those that were previously presented for conventional clamp-on UFMs. First, Section II explains the selection of guided wave mode and the method to excite this required Lamb wave. Section III illustrates the simulation method to simulate a leaky Lamb wave UFM. Then, the effect of surface roughness is quantified and compared with that of conventional UFMs (see Section IV).

II. Leaky Lamb Wave Principle

A. Lamb Wave and Dispersion Curve

Conventional UFMs use bulk waves to analyze the wave propagation (frequency is approximately 1 MHz) within the pipe wall [10], [13]. However, for the leaky Lamb wave UFM, which uses lower frequency (200 kHz) and a longer wavelength, the wavelength is at least twice longer than the pipe wall thickness; therefore, it is better to think of the waves as guided waves. The guided waves are "guided" along one or multiple boundaries between different interfaces. There are usually multiple guided wave modes that can propagate along the structure, and they all travel at different phase velocities, so it is important to recognize and select the modes that are best suited for flow measurements.

The basic principles and analysis of guided waves are well-known [13], [14]. In this article, we only consider the cross section of the pipe. The unwrapping of a pipe into a plate and simplified modeling that results is commonly used to understand guided wave propagation in pipes.

In this article, Disperse [15], a software tool was used to analyze the guided wave modes that may exist in plates and plates immersed in water. Based on the geometry that is modeled, the software assembles a global matrix that contains expressions for partial waves that travel in each layer of a multilayer stack and their respective boundary conditions [16]. The eigenvalues and eigenvectors are then found and related to the wavenumber and mode shape of the modes that can travel along the system.

The software represents the waves in each layer by partial longitudinal and shear waves that leave and enter every layer boundary. Then, the boundary conditions need to be satisfied (continuity for stress and displacement at the boundary) for all boundaries. This will result in four simultaneous equations for this 2-D model (two stress equations and two displacement equations). Assembling these four equations will result in the establishment of a global matrix [16]. Solving for eigenvalues and eigenvectors of this matrix, the wavenumber and mode shape of the modes at different frequencies can be found, respectively.

Consider a simple steel plate, as shown in Fig. 2(a), as an example system. Fig. 2(b) shows the dispersion curve out of Disperse that presents the solutions of $f - k$ on the same plot (where f is frequency, k is the wavenumber, and $d = 5.74$ mm, i.e., the thickness of the modeled plate is the same as that of a DN90 Schedule 40-s pipe).

λ is the wavelength and cp is the phase velocity. It can be seen from Fig. 2(b) that at 200 kHz, two modes exist, A0 and S0, and they are differentiated by different wavenumbers and phase velocity. The mode shapes of these two modes are shown in Fig. 2(c) and (d). The A1 mode (antisymmetrical mode that is one order higher than the A0 mode) starts to appear in the dispersion curve above approximately 300 kHz.

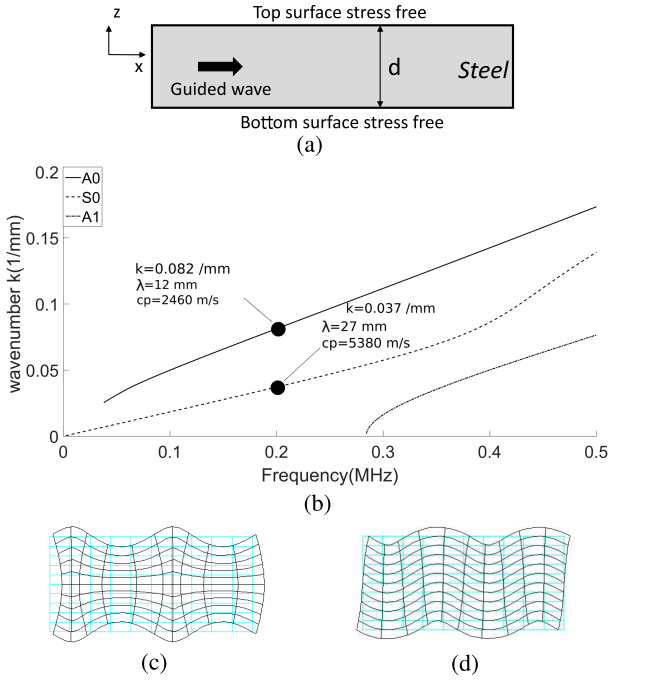

Fig. 2. (a) Cross-sectional view of a 2-D steel plate in a vacuum, the thickness of the steel plate $d = 5.74$ mm. (b) Dispersion curve for a steel plate in a vacuum with a plate thickness of 5.74 mm between the frequencies of 0 and 0.5 MHz. The black points represent modes that exist at 200 kHz. (c) and (d) [16] Mode shape of different modes extracted from Disperse software. S0 represents fundamental extensional mode, and A0 represents fundamental bending mode.

The current operating frequency is 200 kHz; therefore, the A1 mode will not be present and is not discussed further here.

To determine which mode is the more suitable mode to be used in a leaky Lamb wave UFM, plate immersed in a fluid (water, in this case) needs to be analyzed, as shown in Fig. 3(a). The Dispersion curve is shown in Fig. 3(b).

It can be seen that in addition to A0 and S0 modes, the quasi-Scholte mode also exists. However, the quasi-Scholte mode is pinned to the interface [17], and its displacement amplitude decays exponentially with distance from the plate surface. It will not radiate energy far into the fluid of the pipe. Therefore, the quasi-Scholte mode is not suitable to be used in flowmetering.

Compared with S0, A0 is more suitable to be used in flowmetering for two reasons. First, A0 has much higher attenuation along the steel–water interface (attenuation factor for A0 is 88 dB/m, for quasi-Scholte mode 0.007 dB/m and for S0 6.46 dB/m [15]) and, therefore, leaks much more energy into the water. Second, A0 has lower phase velocity in a steel pipe (2460 m/s, more than half the phase velocity of S0, 5380 m/s) and, therefore, can achieve a larger angle of radiation (θ) compared with the S0 mode. This is based on Snell's law (1), where c_w is the phase velocity of water and c_p is the phase velocity of the wave mode propagating in the plate. The lower the c_p, the larger the θ. In addition, using the A0 mode, the radiation angle will also be larger than the conventional flowmeters whose radiation angle is limited by the shear wave velocity (3260 m/s in steel) [18]

$$\sin\theta = \frac{c_w}{c_p}. \tag{1}$$

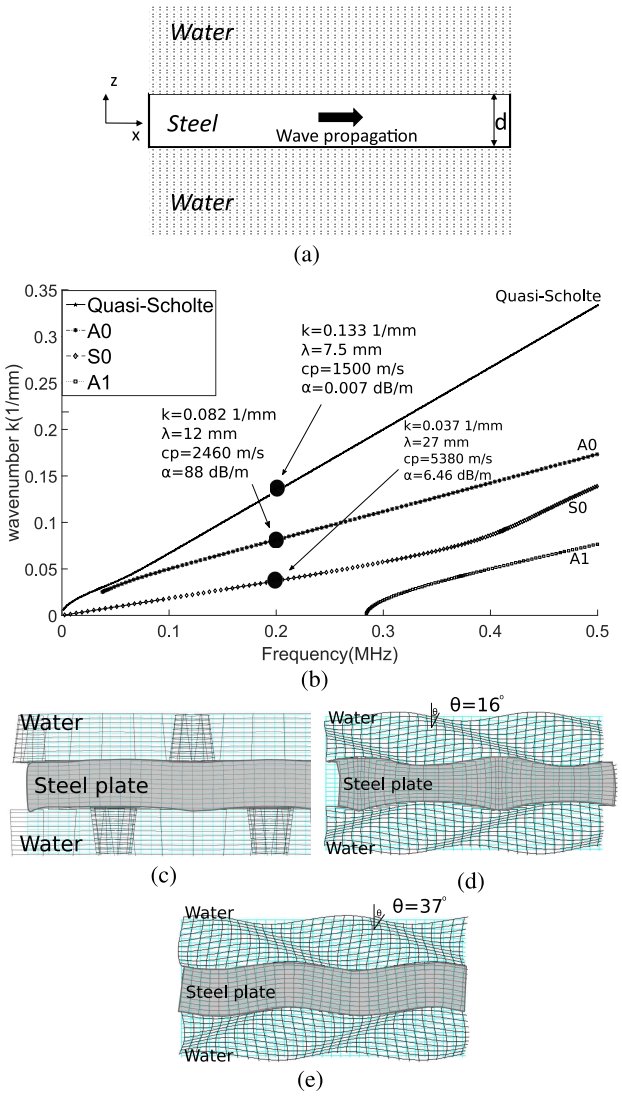

Fig. 3. (a) Cross-sectional view of a 2-D steel plate immersed in water. The thickness of the steel plate $d = 5.74$ mm, and the water sections are both half-space. (b) Dispersion curve for a plate immersed in water with a plate thickness of 5.74 mm between the frequencies of 0 and 0.5 MHz. (c)–(e) [15] The mode shape of different modes extracted from Disperse software. The quasi-Scholte mode is pinned to the interface, S0 represents fundamental extensional mode, A0 represents the fundamental bending mode, and θ represents the wave propagation angle in the water.

Larger radiation angle (larger θ) is beneficial for a flowmeter because it results in a longer time difference between signals that are sent upstream and downstream and, therefore, higher sensitivity to the flow velocity. Hence, A0 is the most suitable mode to be used in flow measurements.

By operating the leaky Lamb wave at 200 kHz, the wavelength of an ultrasonic longitudinal wave in water is 7.5 mm, five times larger than the conventional UFM (wavelength of an ultrasonic wave in water is 1.5 mm) at 1 MHz. The longer wavelength is potentially beneficial to reduce the effect of roughness on measurement uncertainties.

The choice of 200 kHz is based on the following four factors. First, to reduce the roughness-related effects, the frequency chosen should be lower than 1 MHz (used in conventional UFM). Second, at the selected frequency, there

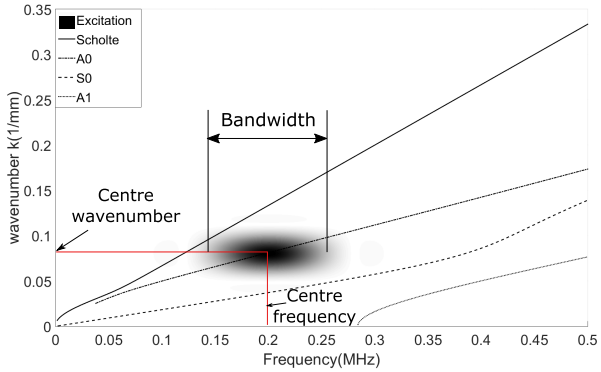

Fig. 4. Dispersion curve for a steel plate immersed in water with a plate thickness of 5.74 mm. Excitation area confined is shown in black, the center frequency of the region is 200 kHz, and the center wavenumber is 0.082 /mm (wavelength of 12 mm).

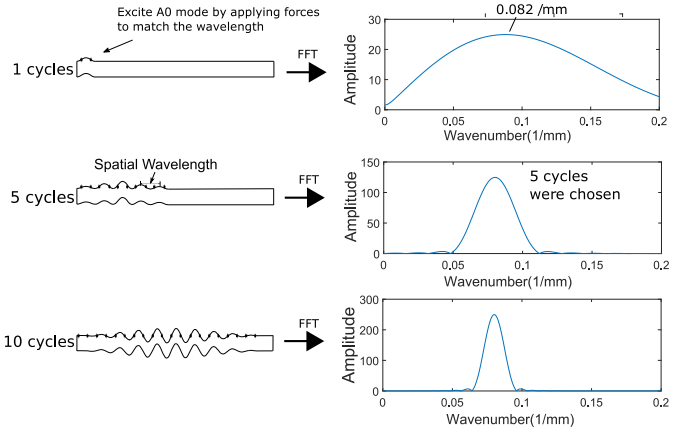

Fig. 5. Spatial variation and FFT for the excitation force for one-, five-, and ten-cycle Hanning windowed tone bursts centered at 0.082 1/mm.

should be a good separation between A0 and other modes so that a pure A0 mode can be excited. Hence, by examining the dispersion curve [see Fig. 3(b)], for frequencies higher than 400 kHz, the separation between S0 and A0 starts to get closer, and A1 starts to appear. For frequencies less than 100 kHz, the nonleaky Quasi-Scholte mode will be partially excited. Hence, the optimum frequency to operate is between 100 and 400 kHz. Third, to maximize the velocity sensitivity, a lower frequency needs to be chosen. The smaller the frequency, the better the velocity sensitivity. Fourth, lower frequency can result in higher uncertainty in the measurement due to random noise. Considering all the above-mentioned factors, 200 kHz is chosen so that good separation between the modes and a balance between velocity sensitivity and the uncertainty caused by random noise is achieved.

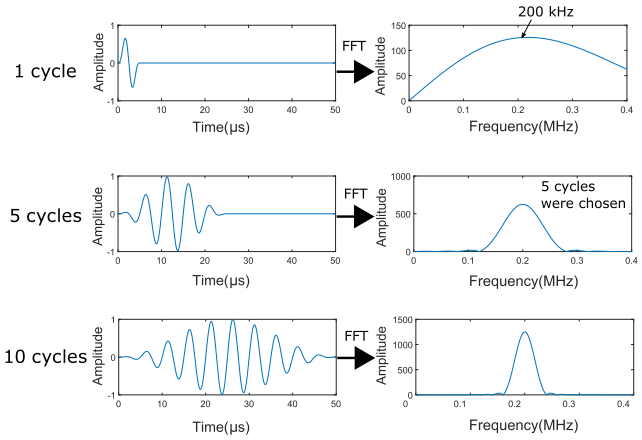

Fig. 6. Time signal and FFT for the horizontal forces in Fig. 5 for one-, five-, and ten-cycle Hanning windowed tone bursts centered at 200 kHz.

B. Excitation of Pure A0 Mode

In practice, a mode that is as pure as possible should be excited so that there are no spurious signals from other modes that make the analysis more difficult. To excite a pure A0 mode at 200 kHz, both frequency and wavenumber (spatial wavelength) of the required mode need to be matched [19]. Fig. 4 shows the dispersion curve. The shaded region indicates the wavenumber (around 0.082 1/mm) and frequency region (around 200 kHz) that the excitation needs to be confined to so that a pure A0 mode is excited. The center frequency and wavelength of this region are 200 kHz and 12 mm, respectively.

To match both the frequency and spatial wavelength of the A0 mode, both the time and spatial force variations of the excitation need to be defined clearly.

To match the spatial wavelength of the A0 mode, the force variation along the pipe is shown in Fig. 5. The wavelength of the spatial force variation is 12 mm. As a result, the center wavenumber of the excitation is 0.082 1/mm. The waveform of a five-cycle Hanning windowed tone burst was chosen for achieving the required spatial bandwidth.

The time signals of the excitation force (force variation versus time) are shown in Fig. 6. It is required that the center frequency of the FFT of the time signal should be equal to 200 kHz. It can also be seen that the waveform of the five-cycle Hanning windowed tone burst is sufficient to achieve the required bandwidth of the excitation region.

III. Simulation Method

A. FE Simulation

Table I shows the parameters of the carbon steel pipe and fluid (water) for the leaky Lamb wave UFM that was modeled.

To implement the finite-element (FE) simulation, the commercial software, Abaqus/Explicit was used. The solver of this software is based on the solutions of the equations of motion for the body using an explicit central difference scheme [20]. The simulation was carried out 2-D, and the pipe is modeled as a plate with the same thickness as the pipe wall thickness, as previously illustrated in Section II. The setup of the FE simulation is shown in Fig. 7. As can be seen, the sets of nodes on the top surface are the transmitter, and the sets on the bottom are the receiver. The concentrated forces are applied on each node of the sets on the top surface as represented by blue arrows. With this loading condition, the A0 mode will be propagating in both directions horizontally along the pipe. Since the problem is symmetric, the symmetry condition

TABLE I

PARAMETERS OF THE REFERENCE CONDITION, STEEL PIPE WITH WATER FLOW INSIDE THE PIPE

Properties	Nominal Value
Pipe properties	
Standard	$3^1/_2$ NPS, SCH 40s
Outer diameter (mm)	101.6
Thickness (mm)	5.74
Material	Carbon steel
Young's modulus (GPa)	217
Material Density (kg/m^3)	7932
Water flow properties	
Temperature (°C)	20
Density (kg/m^3)	998.2
Bulk modulus (GPa)	2.17
Average flow velocity(m/s)	2
Reynold's Number	$1.8x10^5$

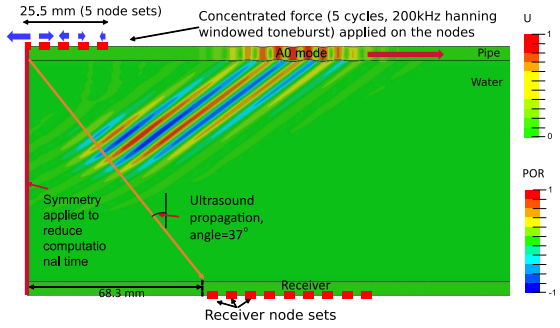

Fig. 7. FE model setup in Abaqus, showing the stress wave in the steel pipe and the pressure wave in the water, 46 μs after the transducer emits the signal. The propagation angle in water is calculated using Snell's law. Legend bar shows the arbitrary color scale of both the magnitude of the displacement (U) in the steel pipe and the acoustic pressure (POR) in water.

TABLE II

ELEMENT AND MESH CHOICE FOR FE SIMULATION

Layer	Steel pipe	Water
Element type	CPE4R	AC2D4R
Mesh size (mm)	0.1	0.25
Minimum wavelength (mm)	12.25	7.4
No. elements per wavelength	122.5	29.6

is applied to reduce the required computational resources to solve the problem.

Table II shows the element and mesh choices used to carry out the simulation. The selection was based on the recommendation by [21] that 15 elements per wavelength should result in accurate modeling. Solid and acoustic elements are used to model the pipe wall and water, respectively. CPE4R is a four-node bilinear plane strain quadrilateral element, and AC2D4R is a four-node linear 2-D acoustic quadrilateral element.

Fig. 8 shows the signal received for all sets of nodes at the receiver. The signals of each of these sets are calculated by adding up the amplitude time history of the nodes that belong to that set. The signals of every second set of nodes were inverted so that the combined signals are constructively added

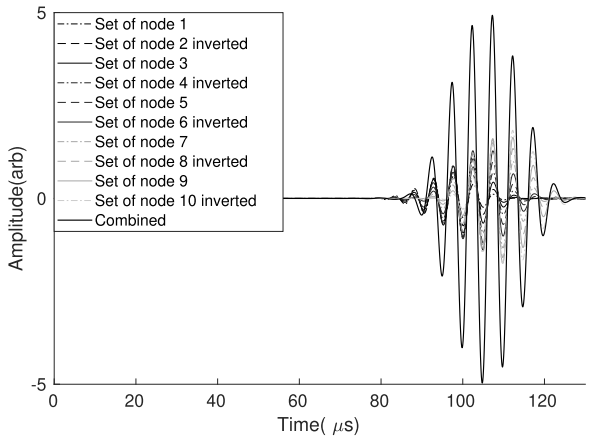

Fig. 8. Simulated signal obtained for each of the ten sets of nodes and summation of the signals from all the sets.

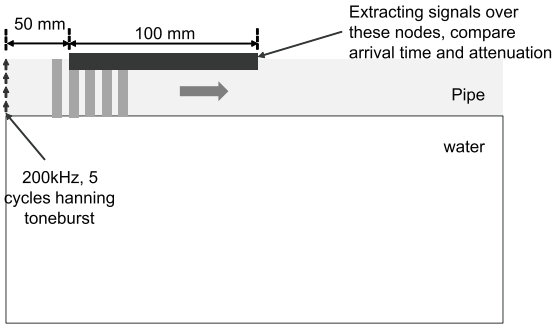

Fig. 9. Steel–water interface model in Abaqus to compare the signals extracted over 100-mm travel length with that of the theoretical obtained signals in Disperse.

up (otherwise, the signals cancel out). Then, the combined signal is the summation of all these ten sets of nodes.

B. Simulation Validation

It is important to verify whether the A0 mode generated in the Abaqus simulation matches those in theoretical calculation. To verify this, a simple FE model that only contains pipe–water interface (see Fig. 9) is built in Abaqus, and the signals obtained from this FE simulation were compared with that of the theoretically obtained values from Disperse [15].

As shown in Fig. 9, the A0 mode is excited by matching the mode shape (u displacement along the pipe thickness). It was assumed that A0 fully develops itself after traveling 50 mm from the source. Then, after A0 has been fully developed itself, signals over 100-mm propagation length are extracted.

Fig. 10 shows the signals extracted from one of these nodes over 100-mm propagation distance after the A0 has been fully developed (after having traveled 50 mm from the source). It can be seen that it is a close match between the simulated signal and theoretical signals.

The maximum amplitude of the signals of the nodes over this 100-mm propagation distance was then extracted and compared with the theoretical maximum amplitude. As shown in Fig. 11, the change in amplitude over 100 mm is a close match between the simulated signal and theoretical signal. The

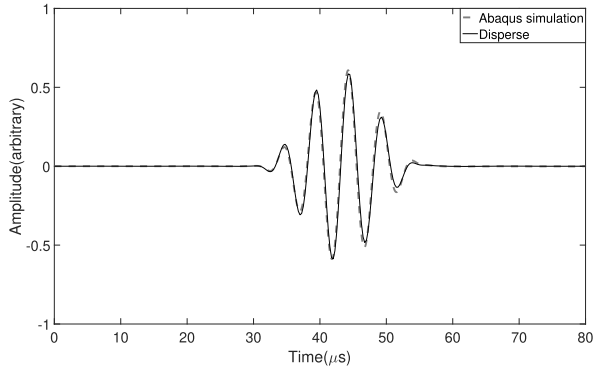

Fig. 10. Signal extracted at one of the nodes within 100-mm propagation distance after A0 mode has fully developed itself and theoretically obtained signal in Disperse.

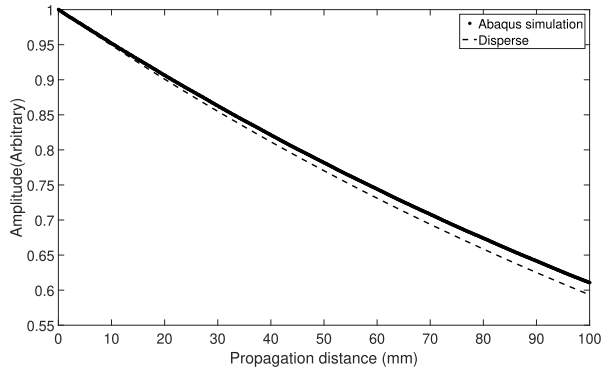

Fig. 11. Amplitude of the signal (both simulated and theoretical) as a function of the propagation distance over propagation distance 100 mm, the starting point of the propagation is after A0 has fully developed itself, 50 mm from the source.

change is slightly smaller for Abaqus, and this may due to the mismatch of the material properties.

C. Flow Simulation

Sections III-A and III-B have explained how to simulate a static leaky Lamb wave UFM. The next step is to add flow simulation to the model. A number of simulation methods have been published to simulate the flow in an UFM [22]–[24]. These methods require large computational resources and time (it might take days to do one simulation). Furthermore, these flow simulation methods focus only on illustrating the effect of the flow on the received signal, whereas this article aims to carry out a parametric study on the effect of the pipe internal roughness on the measurement accuracy of the flow measurements. Hence, in this article, carrying out a detailed CFD modeling on the flow would not be the reasonable choice considering the time and resources it might take. In this case, a quicker and more suitable method without modeling the fluid flow was used. The method is based on considering the overall effect that the flow has on the signal as explained in the following.

As the leaky Lamb wave continuously leaks energy into water, this can be considered as a number of transmitters sending wave packets at the same angle along the pipe. As shown in Fig. 12, the black dotted line represents the

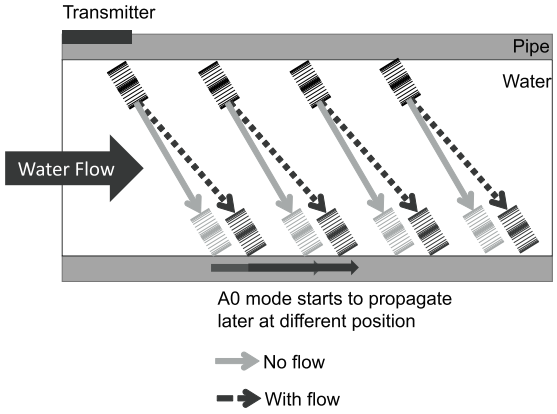

Fig. 12. Effect of the flow on ultrasonic wave propagation in a leaky Lamb wave UFM. The leaky Lamb wave continuously leaks energy to the water. For the first approximation, the phase angle remains the same, while the angle at which the wave packet traverses the pipe changes with the flow.

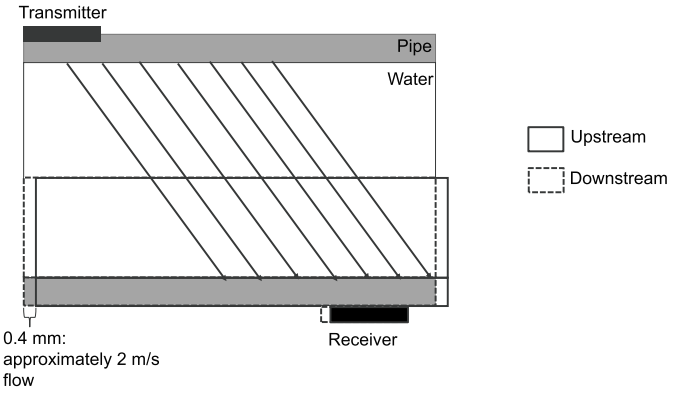

Fig. 13. Movement of the lower part of the model to simulate the flow and shifting the location at which the wave packet arrives on the other side of the pipe.

ultrasonic signal with the existence of flow, while the gray line represents the ultrasonic signal without the flow. It can be seen that the only difference is that with the flow, the angle at which the wave packet traverses the pipe cross-sectional changes. The phase angle of the ultrasonic wave does not change. What this means is that all the wave packets in water will arrive at the other side of the pipe later at a different position (depending on the flow velocity). This results in the transmitted A0 mode also starting to propagate later in a different position. Hence, this means that the ultrasonic signals with the flow can be simulated by moving the lower half of the model to the right. In this case, 0.4-mm movement is approximately equivalent to 2-m/s flow (see Fig. 13 for an illustration). The distance by which the excitation of the transmitted A0 mode is delayed can be described by (2). This method assumes that the phase angle of the ultrasonic wave packets (that arrives from water to the pipe) does not change with or without the existence of the flow. Uniform flow profile is also assumed so that the nonflow profile scattering effect of ultrasound from rough surface can be investigated

$$x = V_f \frac{l_w}{c_w} \tag{2}$$

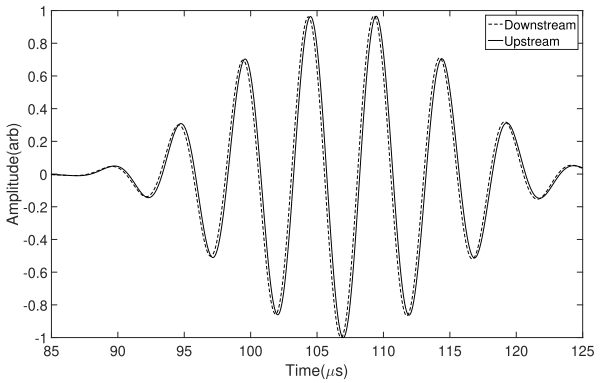

Fig. 14. Simulated downstream and upstream signals.

TABLE III
SIGNAL PROCESSING METHOD TO DETERMINE FLOW VELOCITY FROM THE SIMULATED SIGNALS

Steps	Procedure
1	The upstream and downstream signals are digitally filtered using a 5th order Butterworth filter with cut-off frequency 160KHz and 240KHz.
2	The signal tail which is defined to start 5 cycles after the maximum in signals is removed
3	The upstream and downstream signals are cross-correlated with the sent signal
4	Linear interpolation is used between samples to find the maximum of the cross-correlation function and the arrival time difference (Δt).
5	Calculating the difference between the upstream and downstream arrival time.
6	The flow velocity is calculated using the transit time equation (3).

where V_f is the flow velocity, l_w is the length for ultrasonic wave travel in water, and c_w is the phase velocity of an ultrasonic wave in water.

If the signal, as shown in Fig. 8, is extracted, the upstream and downstream can be obtained. This is shown in Fig. 14.

D. Signal Processing Method to Determine Flow Velocity From Simulated Signals

Table III shows the signal processing steps that were used to calculate the flow velocity from the simulated upstream and downstream signals. From the geometrical features and the measured travel time difference (Δt), the flow velocity v_f can be calculated using the following equation:

$$v_f = \frac{d_i \Delta t}{2 t_u t_d \sin\theta \cos\theta} \tag{3}$$

where v_f is the mean flow velocity, Δt is the difference of the arrival time between t_u (upstream arrival time) and t_d (downstream arrival time), d_i is the internal diameter of the pipe, and θ is the angle between the sound travel path in water and the normal direction. v_f can be determined by combining the individual upstream and downstream travel times that are shown in the following equations:

$$t_u = \frac{d_i}{\cos\theta (c_w - v_f \sin\theta)} \tag{4}$$

$$t_d = \frac{d_i}{\cos\theta (c_w + v_f \sin\theta)} \tag{5}$$

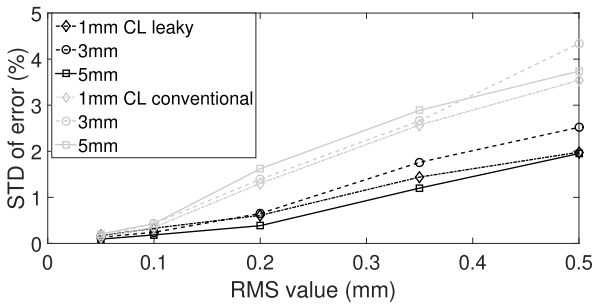

Fig. 15. Standard deviation of the estimated velocity error as a function of rms values and different correlation lengths. For each point plotted, ten realizations were used to estimate the standard deviation that is shown on the graph for both the leaky Lamb wave and conventional UFMs.

where t_u and t_d are upstream and downstream arrival time, c_w is the phase velocity in water, vf is the mean flow velocity, and d_i is the internal diameter of the pipe.

This processing method provides a reference method to process the signals, therefore allowing the parametric study to be performed unbiased.

IV. EFFECT OF SURFACE ROUGHNESS ON MEASUREMENT ACCURACY

To define the surface roughness, two parameters were used. The surface height defines the vertical extent of the roughness profile, and the correlation length defines the horizontal extent [25]. According to [7], the typical rms value for a new pipe is approximately 0.05 mm. This value increases to 0.2 mm for a moderately corroded pipe.

Simulation and experiments have been carried out on the effect of roughness on the conventional clamp-on UFM [6]. In order to make an unbiased comparison with this previous study, the same roughness profiles with the same combination of roughness parameters were used in this article. The rms values chosen are 0.05, 0.1, 0.15, 0.2, 0.35, and 0.5 mm, and the correlation lengths chosen are 1, 3, and 5 mm.

Ten realizations of the roughness profile were produced for each of the combinations of rms value and correlation length. For each profile, the measurement errors were calculated by carrying out simulation explained in Section III. Then, the standard deviations of these ten measurement errors were calculated. This is because even if the parameter combination of the rough surface is the same, the profile that the ultrasound transmits through is different. Hence, to quantify the effect of roughness, the standard deviation of measurement errors of these ten realizations is calculated.

As shown in Fig. 15, for pipe wall with rms values less than 0.1 mm, the absolute standard deviations of error for both UFMs are relatively small. There is a small improvement for leaky Lamb wave UFM, but there is no clear separation between the leaky Lamb wave UFMs and conventional UFMs. However, for rms values larger than 0.1 mm, the effect of roughness on measurement accuracy has been clearly reduced for all combinations of roughness parameters when using the leaky Lamb wave UFMs. The standard deviation of error was reduced from approximately 4% to 2% for rms value 0.5 mm.

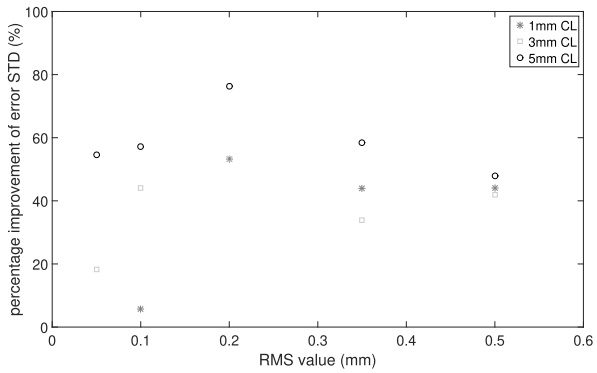

Fig. 16. Percentage improvement of STD of error as a function of rms value and correlation length for leaky Lamb wave UFMs compared with conventional UFMs.

Fig. 16 shows the percentage improvement of this standard deviation of error at each rms value and correlation length.

It can be seen that using leaky Lamb wave UFMs, the roughness-related uncertainties are reduced by approximately 50% compared with conventional UFMs for rms values larger than 0.1 mm (0.2, 0.35, and 0.5 mm).

V. Demonstration Experiments to Generate and Receive Leaky Lamb Wave

Experiments were carried out to verify that this leaky Lamb wave method is suitable for flow measurements and that a pure A0 mode can be generated. Section V-A illustrates the use of an electromagnetic acoustic transducer (EMAT) to transmit the A0 mode and the use of shear elements to receive the ultrasonic signals. Section V-B shows the verification of the presence of the excited A0 mode in a dry pipe using the 2-D fast Fourier transform (2-D FFT). Finally, Section V-C illustrates the leaky A0 signals received for pipe filled with water.

A. EMAT Transmitter and Shear Receiver

To generate the A0 mode in the pipe wall, as shown in Fig. 5, EMATs were used so that the whole circumferential surface of the pipe can be excited (strictly speaking, pipe modes should be considered rather the A0 modes existed in a plate. However, as explained in Section II, for simplicity, the discussion will continue as if the pipe is unrolled into a plate and will refer to the flexural motion of the pipe wall as the A0 mode. This is commonly used to understand the guided wave propagation in pipes). Fig. 17(a) shows the operating principle of EMAT. The distance between the electric wires is half the spatial wavelength of the A0 mode. The electric current through the electric wires is set to be a 200-kHz, five-cycle Hanning windowed tone burst. The current produces eddy currents on the surface of the pipe, which interacts with the bias magnetic field to produce a force pattern on the surface of the pipe due to the Lorentz force.

A schematic of the cross-sectional view of the EMAT on the pipe wall is shown in Fig. 17(b). Electrical wires were wound around the pipe. There are a total of ten magnets evenly distributed around the circumference. The number of magnets

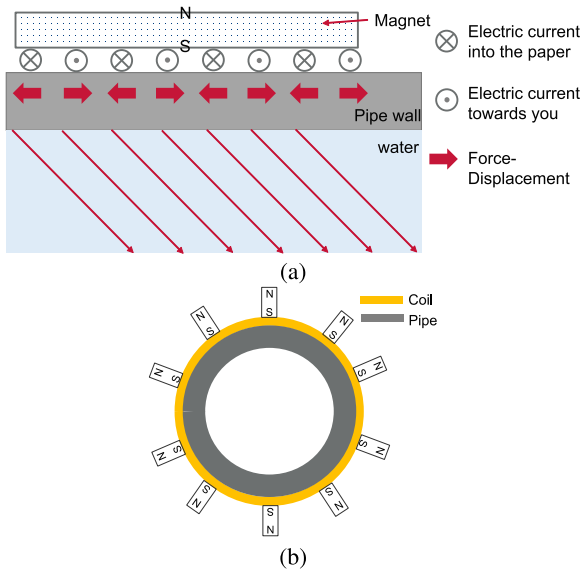

Fig. 17. (a) Principle of EMAT and the generation of the Lorentz force on the pipe wall to match the frequency and wavenumber of A0 mode. (b) Schematic of the cross-sectional view of EMAT on the pipe wall.

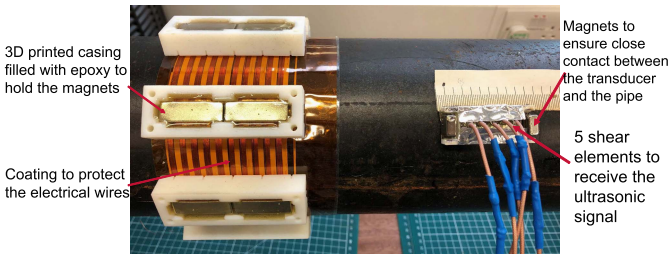

Fig. 18. Photograph of the setup in the laboratory. EMAT patches were used to transmit A0 mode, piezoelectric transducer containing five piezoelements was used to receive the signal, and the transducer was placed approximately 150 mm away from the EMAT patches.

that need to be placed around the pipe to reduce the effect of higher order modes is studied in [26] and [27]. More details of the design of EMAT and the principle of generating ultrasonic waves using EMAT can be found in [28].

Fig. 18 shows the transducer setup along the pipe. The electrical wires used in EMAT are of 0.2-mm diameter, and there are ten turns of wires in each patch. The magnets ($30 \times 10 \times 5$ mm-thick N42 Neodymium Magnet, F30105-4, first4magnets, U.K.) were contained within a 3-D printed casing filled with epoxy. To receive the A0 mode generated by the EMAT, a shear transducer with five piezoelectric elements were used. The piezoelements (NCE51 5 mm^2 $\times$ 1 mm thickness, Noliac, U.K.) were 6 mm (half the A0 wavelength) apart, and they were contained within a 3-D printed casing. The magnets were installed to ensure close contact between the elements and the pipe. Treacle was used as a coupling material. The receiver transducer was placed approximately 150 mm away from the EMAT patches. For electrical setup, the Handyscope HS5 (Tiepie Ltd., Sneek, The Netherlands) was used to transmit (200-kHz, five-cycle tone burst, 12 V) and receive (14-bit ADC at the 50-MHz sampling frequency) ultrasonic signals. The power amplifier

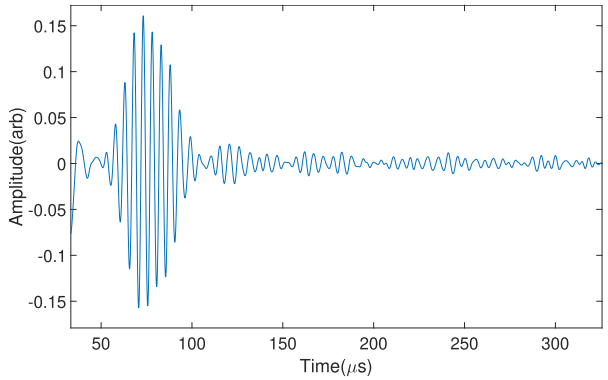

Fig. 19. Signals received using the piezoelectric transducer receiver. The signals are the summation of the signals from all the five elements.

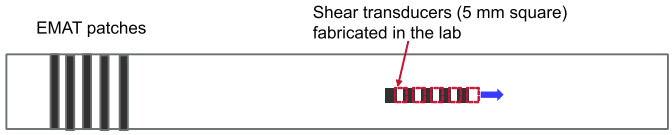

Fig. 20. Schematic to illustrate the setup along the length of the pipe. EMAT patches were used to transmit A0 mode, and shear piezoelectric transducers were used to receive the signal. There is no water in the pipe. To verify the mode, 2-D FFT was performed by moving the shear elements to 64 equally spaced positions between the propagating distances of 300 and 428 mm away from the EMAT patches.

(Yamaha Natural Sound Integrated Amplifier, A-S500, Japan) amplifies the transmission input signal by 20 dB, and the preamp amplifies the receiver output signal by 60 dB. The signal received by shear elements (the sum of the signals from five elements) is shown in Fig. 19.

B. A0 Mode Validation in a Dry Pipe

To validate that the desired pure A0 mode was generated by the EMAT patches, 2-D FFT was used. This method transformed the received amplitude–time record (measured at different locations along the pipe) to amplitude wavenumber records at discrete frequencies [29], [30], where the individual Lamb wave mode can be recognized. The schematic setup along the length of the pipe is shown in Fig. 20.

The amplitude–time signals were recorded at 64 equally spaced positions between propagating distance of 300 and 428 mm away from the EMAT patches. The reason for placing the transducer at more than 300 mm away from the transmitting EMAT is for the A0 mode to fully develop along the pipe. In addition, the pipe was not filled with water to ensure that the shear elements only receive A0 mode traveling along the pipe (no leaky A0 as there is no water). Fig. 21 shows the 2-D FFT results displaying the wavenumber-frequency relationship of the signals. It can be seen that the amplitude reaches a maximum at the wavenumber corresponding to A0 mode at 200 kHz. This amplitude is at least 20 dB more than the rest of the mode so it can be concluded that a pure A0 mode was excited by the EMAT. It also shows good agreement with the predicted region of excitation (see Fig. 4).

C. Leaky A0 Validation

After verifying that, the A0 mode is transmitted along the pipe. The next stage is to fill the pipe with water and examine

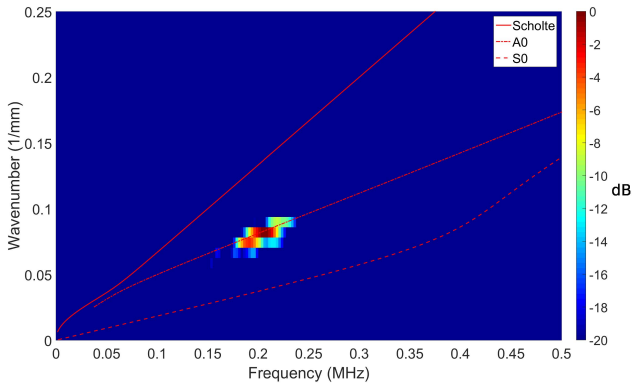

Fig. 21. 2-D FFT results displaying the wavenumber-frequency relationship of the signals. The Dispersion curve for the 5.74-mm thickness plate is also shown.

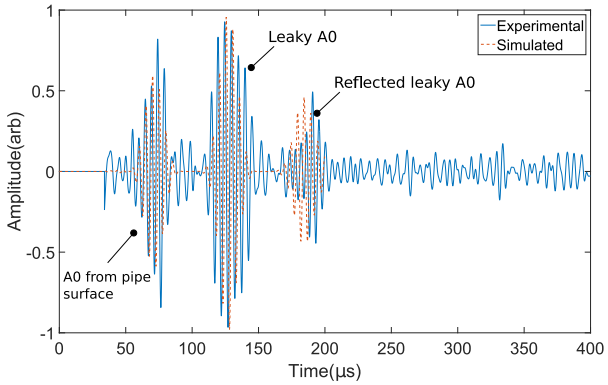

Fig. 22. Signals received for experimentally obtained signals using EMAT as the transmitter and piezoelements on pipe to receive signals. The pipe was sealed at both ends and filled with water. Simulated signals in Abaqus are also shown. The simulation setup is the same as that in Fig. 7 except that the same concentrated forces were also applied on the lower side of the pipe wall.

the leaky Lamb wave. The setup was the same as that in Fig. 18 except that the pipe was sealed at both ends and was filled with water.

Fig. 22 shows the signals received by the shear piezoelements and the signals simulated in Abaqus. The simulation setup is the same as that in Fig. 7 except that the same concentrated forces were also applied on the lower side of the pipe wall. It can be seen that the arrival time of the A0 and leaky A0 matches with the simulation signal. However, the SNR for this acquisition is not ideal. This can be improved by better-constructed transducer system (printed circuit board instead of manually winding wire, better alignment of the transducer, amplifier with less noise, and more piezoelement transducer to receive the signals around the circumference of the pipe). In addition, there might also be coherent noise due to 3-D guided wave modes that have not been modeled in 2-D simulation.

VI. Conclusion

This article investigated the nonflow profile-related effect of roughness on the measurement uncertainties of the leaky Lamb wave-type UFMs. This leaky Lamb wave method uses

longer wavelength and lower frequency (200 kHz, approximately five times lower than the conventional UFMs) than the conventional UFMs. The ultrasonic signals were simulated using Abaqus, and then, these simulated signals were used to calculate the roughness (only pipe wall roughness with rms value up to 0.5 mm has been modeled) related uncertainties. It was found that the error of leaky Lamb wave UFM caused by roughness is approximately half of that of conventional UFMs for corroded pipes with rms values larger than 0.1 mm (0.2, 0.35, and 0.5 mm). Since for conventional UFMs, roughness can be the most important contributor to the stated 1%–5% measurement errors, the prospect of halving these errors by using a lower frequency leaky Lamb wave UFMs is attractive. Demonstration experiments were also carried out to verify that the pure A0 mode can be transmitted using an EMAT transducer. The experiments also successfully detected the leaky A0 mode and demonstrated all the wave propagation physics that is adequately captured in the simulation.

ACKNOWLEDGMENT

The authors wish to acknowledge the support of ABB that provided useful background knowledge with respect to industrial flowmeters.

REFERENCES

[1] R. C. Baker, *Flow Measurement Handbook: Industrial Designs, Operating Principles, Performance, and Applications*. Cambridge, U.K.: Cambridge Univ. Press, 2000.

[2] L. C. Lynnworth and Y. Liu, "Ultrasonic flowmeters: Half-century progress report, 1955–2005," *Ultrasonics*, vol. 44, pp. e1371–e1378, Dec. 2006.

[3] M. L. Sanderson and H. Yeung, "Guidelines for the use of ultrasonic non-invasive metering techniques," *Flow Meas. Instrum.*, vol. 13, no. 4, pp. 125–142, Aug. 2002.

[4] J. M. Szebeszczyk, "Application of clamp-on ultrasonic flowmeter for industrial flow measurements," *Flow Meas. Instrum.*, vol. 5, no. 2, pp. 127–131, Apr. 1994.

[5] M. Cermakova, J. Kris, O. Cermak, and J. Bozikova, "Uncertainty in the measurements of clamp-on ultrasonic flowmeters," *Slovak J. Civil Eng.*, vol. 1, pp. 7–12, 2004.

[6] X. Gu and F. Cegla, "The effect of internal pipe wall roughness on the accuracy of clamp-on ultrasonic flowmeters," *IEEE Trans. Instrum. Meas.*, vol. 68, no. 1, pp. 65–72, May 2018.

[7] *NORSOK STANDARD P-001, Process Design*, Norwegian Petroleum Indsutry, Lysaker, Norway, 2006, p. 9.

[8] D. Benstock, F. Cegla, and M. Stone, "The influence of surface roughness on ultrasonic thickness measurements," *J. Acoust. Soc. Amer.*, vol. 136, no. 6, pp. 3028–3039, Dec. 2014. [Online]. Available: http://asa.scitation.org/doi/10.1121/1.4900565

[9] L. C. Lynnworth and T. H. Nguyen, "Leaky Rayleigh wave clamp-on flowmeter," in *Proc. IEEE Ultrason. Symp.*, Waltham, MA, USA, 1985, pp. 519–524.

[10] H. Sato, M. Lebedev, and J. Akedo, "Theoretical investigation of guide wave flowmeter," *Jpn. J. Appl. Phys.*, vol. 46, no. 7B, pp. 4521–4528, Jul. 2007.

[11] Flexim. *FLEXIM Gas Flow Meters: Shear Waves and Lamb Waves*. Accessed: Mar. 4, 2019. [Online]. Available: http://www.flexim.ro/gasultrasonicflowmeter_principle.php.htm

[12] D. Jim. *Simens SITRANS F US: Strength in Numbers: Matching Lamb Wave Sensors to the Resonant Frequency of a Pipe Wall*. Accessed: Apr. 3, 2019. [Online]. Available: https://www.flowcontrolnetwork.com/strength-in-numbers/

[13] J. L. Rose, *Ultrasonic Waves in Solid Media*. Cambridge, U.K.: Cambridge Univ. Press, 1999.

[14] K. F. Graff, *Wave Motion in Elastic Solids*. New York, NY, USA: Dover, 1975.

[15] M. J. S. Lowe and B. N. Pavakovic, "Disperse user manual, version 2.0.11d," Imperial College Sci., Technol. Med., London, U.K., Tech. Rep., 2001. Accessed: Mar. 4, 2019. [Online]. Available: https://www.imperial.ac.uk/nde

[16] M. J. S. Lowe, "Matrix techniques for modeling ultrasonic waves in multilayered media," *IEEE Trans. Ultrason., Ferroelectr. Freq. Control*, vol. 42, no. 4, pp. 525–542, Jul. 1995.

[17] F. B. Cegla, P. Cawley, and M. J. S. Lowe, "Material property measurement using the quasi-scholte mode—A waveguide sensor," *J. Acoust. Soc. Amer.*, vol. 117, no. 3, pp. 1098–1107, Mar. 2005.

[18] J. Han, H. Liu, Y. Zhou, R. Zhang, and C. Li, "Studies on the transducers of clamp-on transit-time ultrasonic flow meter," in *Proc. 4th IEEE Int. Conf. Inf. Sci. Technol.*, Apr. 2014, pp. 1–4.

[19] P. D. Wilcox, "Lamb wave inspection of large structures using permanently attached transducers," Ph.D. dissertation, Imperial College Sci., Technol. Med., London, U.K., 1998.

[20] *Abaqus Documentation 6.14*, Dassault Syst. Simulia Corp., Providence, RI, USA, 2014.

[21] M. B. Drozdz, "Efficient finite element modelling of ultrasound waves in elastic media," Ph.D. dissertation, Imperial College Sci. Technol. Med., London, U.K., 2008.

[22] J. Reyes, C. D. Desarrollo, G.-M. Student, and A. Acevedo, "Simulation and experimental validation of a transit time in an ultrasonic gas flow meter using air," in *Proc. ANDESCON*, 2010, pp. 1–6.

[23] P. C. Eccardt, H. Landes, and R. Lerch, "Finite element simulation of acoustic wave propagation within flowing media," in *IEEE Ultrason. Symp.* Linz, Austria: Simens AG German and Univ. of Linz, 1996, pp. 991–994.

[24] A. Luca, K. Fodil, and A. Zerarka, "Full-wave numerical simulation of ultrasonic transit-time gas flowmeters," in *Proc. IEEE Int. Ultrason. Symp. (IUS)*, no. 2, Sep. 2016, pp. 1–4.

[25] *Geometrical Product Specifications (GPS)-Surface Texture: Profile Method-Terms, Definitions and Surface Texture Parameters*, Standard EN ISO 4287:1998, ISO 4287:1997.

[26] B. Herdovics and F. Cegla, "Structural health monitoring using torsional guided wave electromagnetic acoustic transducers," *Struct. Health Monit., Int. J.*, vol. 17, no. 1, pp. 24–38, Dec. 2016.

[27] H. Nishino, S. Takashina, F. Uchida, M. Takemoto, and K. Ono, "Modal analysis of hollow cylindrical guided waves and applications," *Jpn. J. Appl. Phys.*, vol. 40, no. Part 1, No. 1, pp. 364–370, Jan. 2001.

[28] M. Hirao and H. Ogi, *Electromagnetic Acoustic Transducers: Noncontacting Ultrasonic Measurements Using EMATs* (Springer Series in Measurement Science and Technology), 2nd ed. Toyonaka, Japan: Springer, 2017.

[29] D. N. Alleyne and P. Cawley, "A 2-dimensional Fourier transform method for the quantitative measurement of Lamb modes," in *Proc. IEEE Symp. Ultrason.*, Dec. 1990, pp. 1143–1146.

[30] F. B. Cegla, "Energy concentration at the center of large aspect ratio rectangular waveguides at high frequencies," *J. Acoust. Soc. Amer.*, vol. 123, no. 6, pp. 4218–4226, Jun. 2008.

Xiaotang Gu received the M.Eng. degree in mechanical engineering from Imperial College London, London, U.K., in 2015, where he is currently pursuing the Ph.D. degree with the Dynamics and Non-Destructive Evaluation (NDE) Group, Mechanical Engineering Department.

Frederic Cegla was born in Freiburg im Breisgau, Germany. He received the M.Eng. and Ph.D. degrees in mechanical engineering from Imperial College London, London, U.K., in 2002 and 2006, respectively.

He returned to Imperial College London after a short stay as a Post-Doctoral Research Fellow at The University of Queensland, Brisbane, QLD, Australia. He is currently a Senior Lecturer (Associate Professor) and an EPSRC Research Fellow with the Non-Destructive Evaluation (NDE) Group, Imperial College London. He was the Founder of Permasense Ltd., London, a spin-out company and a market leader in the field of wireless ultrasonic corrosion monitoring. He has authored more than 50 publications. He holds six patents. His current research focuses on the topics of ultrasonic sensors, ultrasonic monitoring techniques, structural health monitoring, and ultrasonic manipulation of particles and bubbles.